White Paper

Sequential Peeling: a Model-Based Approach to Structure Identification and De-embedding

Dozens of different network extraction and de-embedding methods exist (e.g., [1]-[7]) for different measurement environments. Some take a black-box approach to the fixture or mounting assembly and try to determine its S-parameters, as accurately as possible, through measurements of standards and making some assumptions about the structure (e.g., reciprocity, symmetry, degree of mismatch, etc.). Another approach is model-based where it is assumed that a portion of the fixture has a specific circuit configuration (e.g., a transmission line, a series impedance, etc.). This paper is about one of those model-based approaches that uses position information about structures in the fixture, and an indicated impedance/admittance model to extract parameters of that particular structure. Since position information is used, one structure can be de-embedded after another. In a sense, this is peeling away one layer of the fixture at a time which is the source of the name of the method.

The process involved in this method will be discussed in this paper along with the assumptions being made and the sensitivities that might be encountered.

The concepts

Even within the peeling class, there are many variations of methods (e.g., [7]-[8]) where some treat the problem as a sequence of black boxes and others aim for a detailed circuit model generation. The version being discussed here is somewhere in the middle in that models will be used in the generation but they will be somewhat abstract with the main aim of capturing the dominant physical behavior of the transition.

The premise behind a measurement/modeling approach like sequential peeling is that the fixture can be broken down into simple lumped elements, possibly separated by transmission lines, (see Figure 1) and that these elements can be found through measurement. A pure modeling approach might use EM simulation to evaluate those elements but, in practice, it might be difficult to obtain the needed accuracy due to complexity of the materials or the geometry or due to proper handling of radiative effects.

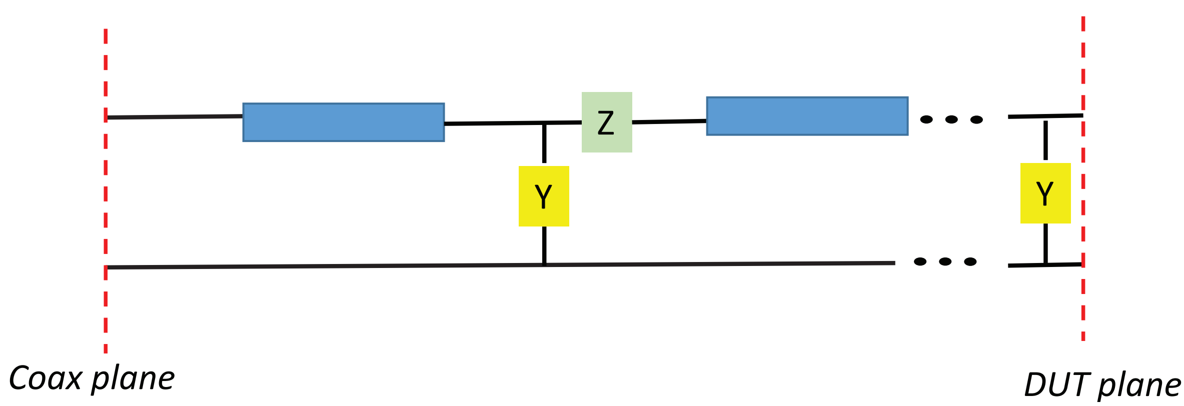

Figure 1. A semi-lumped model of a fixture that is amenable to a technique such as sequential peeling is shown here.

The lumped elements might physically be vias, abrupt transitions, line bends, close approaches of nearby metallization or other structures. The important requirement is that they be electrically small (compared to the frequency range being analyzed) and one can assign a shunt or series nature to them. For other structure types, a black-box approach (or at least a different modeled approach) may be a better choice. The sequential peeling approach does not require a net list and is not trying to solve for circuit elements explicitly but rather it is attempting to come up with a simple model that does a reasonable job of describing fixture behavior while being able to extract those model elements with sufficiently simple measurements. Other methods exist that take a more discrete approach to circuit evaluation that are valuable for other purposes and are not covered here.

The process and the calculations

The basic process involves finding a dominant electrical length position to study (i.e., the location of the structure of interest). The user can enter this directly or (by entering 0), the system will automatically find the dominant length. This chunk is then isolated to create a subset S-parameter describing that zone. Now, this subset S-parameter may include residual effects of other structures and the complete set of S-parameters for the structure may not be self-consistent so this is where the modeling comes in. The user will have selected a shunt-Y or series-Z behavior as the form of interest and that element is solved for by inverting one on the below equations (Z_0 is the reference impedance; this is by default the reference impedance of the calibration but it can be transformed to another impedance by the instrument).

Series Z:

$$S_{11} = S_{22} = \frac{Z}{2Z_0 + Z}$$

$$S_{21} = S_{12} = \frac{2}{2 + Z / Z_0}$$

Shunt Y:

$$S_{11} = S_{22} = \frac{-YZ_0}{2 + YZ_0}$$

$$S_{21} = S_{12} = \frac{2}{2 + YZ_0}$$

Once the Z or Y element is found (and it will be a function of frequency), the .s2p file for the structure is then found by applying the appropriate equations above in the forward direction. This creates the self-consistent set of S-parameters that avoids causality and other issues with the structure's network description.

For a differential structure, the principle is basically the same except the only allowed model is a cross-bar impedance (if series elements or elements to ground are needed, the two-port method described above can be applied to four port measurement data) and the analysis is applied to a mixed mode parameter such as S_{d1d1}. From a differential reflection (phase-isolated as discussed before), one can calculate the impedance value by inverting

$$S_{dd} = \frac{-Z_0}{Z + Z_0}$$

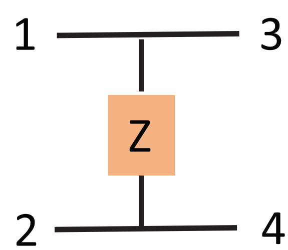

Figure 2. The model element for a mixed-mode parameter using the sequential peeling method is shown here. Four port and differential structure de-embedding approaches can also include series and shunt-to-ground models using the single-ended S-parameters and the process described above. The port numbering shown here is for the S-parameter equations in the text but they will be dynamically assigned in practice based on the mixed-mode parameter being used.

The .s4p file based on the model can then be generated from the following (where the port numbering matches that shown in Fig. 2):

$$S_{11} = S_{22} = S_{33} = S_{44} = \frac{-Z_0}{2 \cdot (Z + Z_0)}$$

$$S_{31} = S_{13} = S_{42} = S_{24} = \frac{2 \cdot Z + Z_0}{2 \cdot (Z + Z_0)}$$

$$S_{41} = S_{14} = S_{21} = S_{12} = S_{23} = S_{32} = S_{43} = S_{34} = \frac{Z_0}{2 \cdot (Z + Z_0)}$$

Once this first structure has been found, it can be de-embedded using the instrument's embedding/de-embedding engine ([9], chapter 10) and then the process repeated for the next most significant structure. This is where the 'peeling' term comes from. Note that there are some limits to this:

- When a large reflection occurs early in the fixture, this substantially reduces the available signal-to-noise ratio for identifying later structures and accuracy on those secondary structure may suffer. This hampers most extraction algorithms to some extent since one is trying to 'look through a brick wall' in some sense.
- If structures are closer together than about 5/(frequency sweep range), the resolution capability will suffer and the simple Y and Z modeling may fail. Similarly, if the frequency point density is so coarse that phase wraps might be missed, the localization capability can fail and the model extraction may also be inaccurate. Warnings are issued in these cases.

- The method assumes that the fixture basic impedance is relatively close to the reference impedance ('close' depends on the reflection levels of the structures of interest, 10% for larger reflections). If this is not the case, one of the black-box extraction methods ([9]; chapters 8 and 22) might be a better choice.
- When doing a peeling strategy, often one must also remove transmission line sections in practice. The particular method described here does not identify transmission line sections (since they are electrically long by definition) but other tools are available to help. One of the simpler ones is an auto-ref-plane-with-loss technique that is discussed in the MS464XB Calibration and Measurement Guide [9]. One can also use fixture dimension and materials information to de-embed transmission line lengths directly using the embedding/de-embedding engine ([9], chapter 10).

There are many ways one could explore the various uncertainty mechanisms in this process. It is beyond the scope of this paper to be exhaustive but the effect of nearby reflective structures warrants some additional discussion. As with time domain analysis or any kind of phase resolution study, there is a limit if electrical lengths of interest are too similar on the scale of 1/(frequency span). One can look at the added induced error on extracted low frequency match as this scaling is changed (in this case by scaling the frequency range but the principle holds in general if loss is held constant). The structure of interest has a return loss of about 30 dB (0.03 linear reflection magnitude) and the nearby structure has about the same reflection level and the loss between them is low. The error relative to a distant spacing is plotted in Figure 3 as a function of the product of the spacing in time and the frequency sweep range used. As that product dips below about 5, the error is a substantial fraction of the reflection coefficient of interest and may be objectionable.

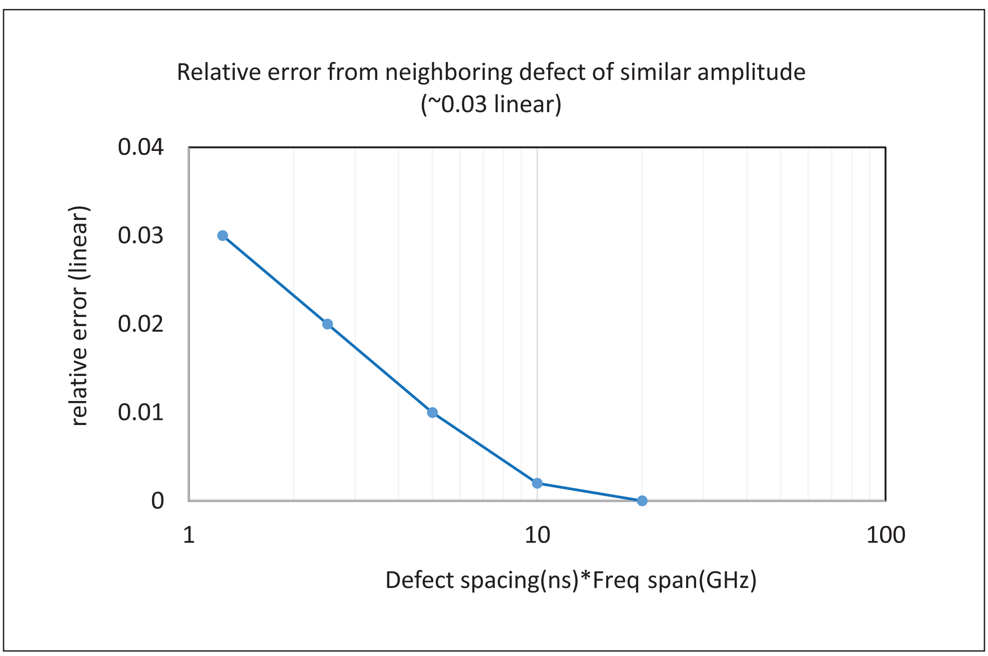

Figure 3. The effect of a neighboring structure on the extracted low frequency reflection of a structure of interest (mean value =0.03 at 1 GHz) is plotted here versus a spacing variable

Handling the transmission line sections is another topic of interest and an additional feature in sequential peeling allows the extracted network to be compensated for losses from those transmission line segments (and other items) earlier in the fixture. Since an isolated structure is used for the extraction, there is in general little information about loss before that structure so the extracted model may appear artificially well-matched (or lower loss). With the use of a reflect standard at the end of the fixture, the system will have the ability to estimate total loss and scale it for the position of the extracted structure. The magnitude of the reflection coefficient of the standard must be known (and an average over the frequency range should be employed if the magnitude is varying) and it is assumed that the majority of the loss is uniformly distributed along the length of the fixture. Generally an open or a short for the reflection standard is recommended for maximum accuracy (particularly as the fixture loss exceeds ~5-10 dB) and accuracy will degrade regardless if the fixture loss exceeds about 15 dB since system residual directivity will limit the measurement anyway. Base calibrations with better residual directivities (e.g., AutoCal or TRL/LRL or s1p-based defined-standards calibrations) will maximize the usable range. If the loss is high and very non-uniform, other network extraction techniques are recommended ([9]; chapters 8 and 22).

As an example, consider a via embedded in a long fixture and the desire is to extract a model-based file for that via. If one proceeded directly, the extracted match of the via would be the solid curve in Fig. 4. Using an open reflect standard to assist, however, produces the dashed curve in that figure. Ignoring the preceding loss in the fixture resulted in an over-estimation of via return loss by nearly 10 dB at 26 GHz. This is admittedly an extreme case (based on fixture length) but the reflect standard, if available, can enable a useful correction.

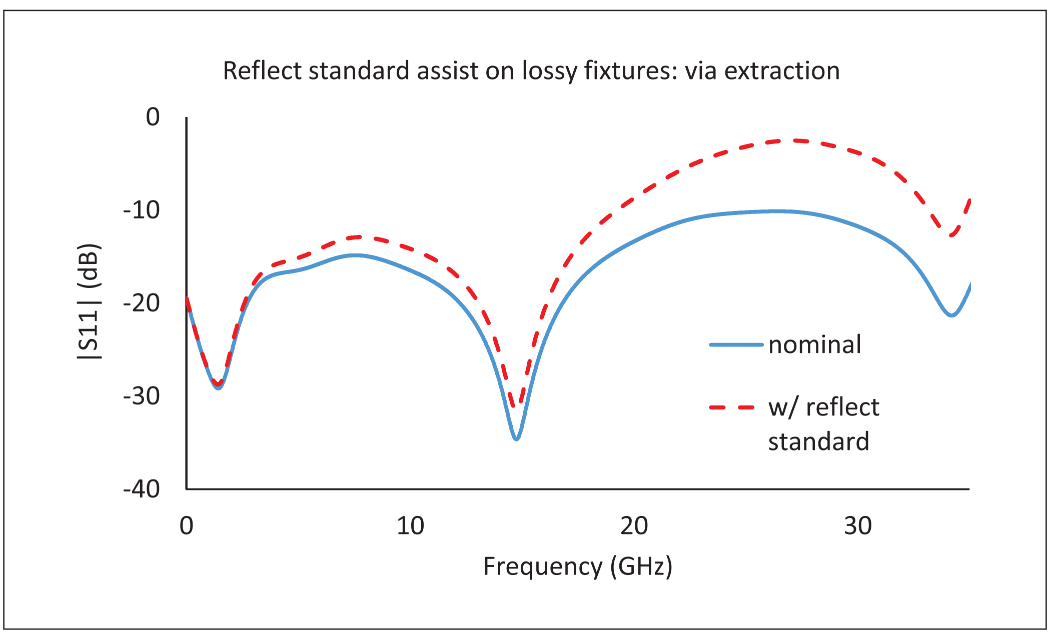

Figure 4. The extracted match of a via structure in a fixture is plotted here without ('nominal') and with a reflect-standard-based correction for fixture loss.

Examples and analysis

To place these concepts and processes into context, an example may be useful. Consider a fixture that has a coaxial launch, a via transition in the middle and then another launch to the DUT plane. The desire is to measure the return loss of a relatively well-matched DUT (around 15 dB return loss between 10 and 20 GHz). The structure of the fixture is shown in Fig. 5. The time domain impulse response of the fixture with the DUT plane left open (as viewed from the coax plane) is shown in Fig. 6.

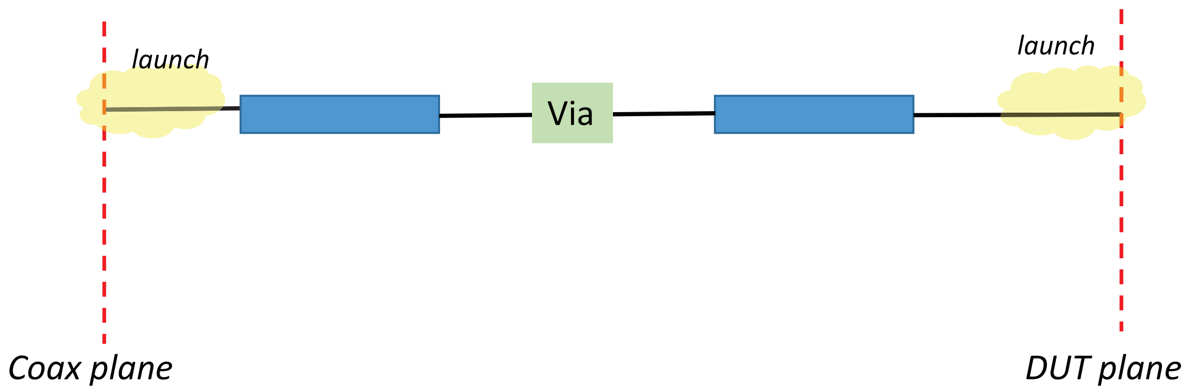

Figure 5. The fixture structure for the example is illustrated here.

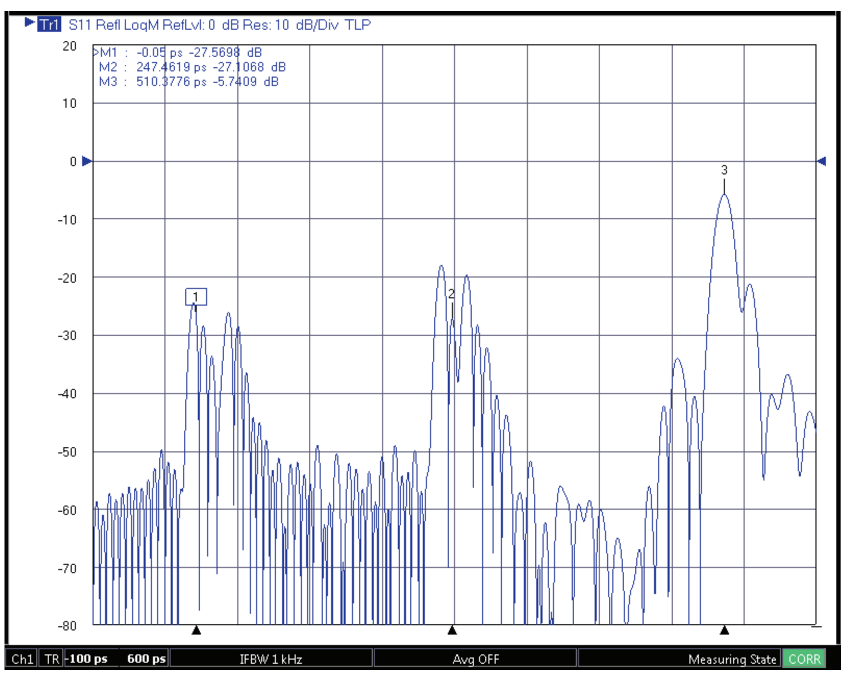

Figure 6. The time domain impulse response (viewed from the coax connector) of the fixture structure in Figure 5 is plotted here. The DUT plane was left open

The coaxial launch signature is visible near time=0 (marker 1) and the via signature is visible near marker 2. A combination of the DUT launch and the open radiation pattern forms the large structure near marker 3. One might be tempted to conclude that the value of marker 3 (around –5.7 dB) gives some indication of double the insertion loss of the fixture but the radiative impedance of the DUT plane was actually not that close to a true open.

If one looks at the measurement data in Figure 7 (calibration at the coaxial plane, DUT in place at the DUT plane), one sees reflection coefficients that are higher than expected (particularly mid-band).

A first step might be then to use the peeling approach to evaluate the launch. It was not known *a priori* if this defect was more shunt-like or series-like so both were evaluated (Figure 8). In this case, it is relatively easy to see from the extracted defect S-parameters that a shunt (Y)-like model is more physical just based on passivity. The insertion loss does start to decrease slightly at higher frequency due to some compensation in the launch layout.

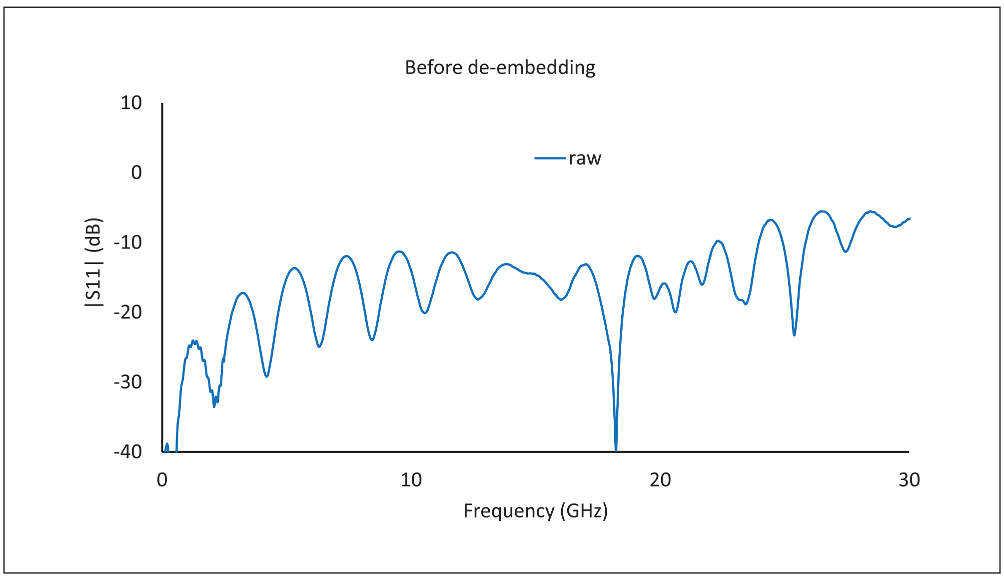

Figure 7. The (unextracted) measured data of the fixture + DUT is plotted here.

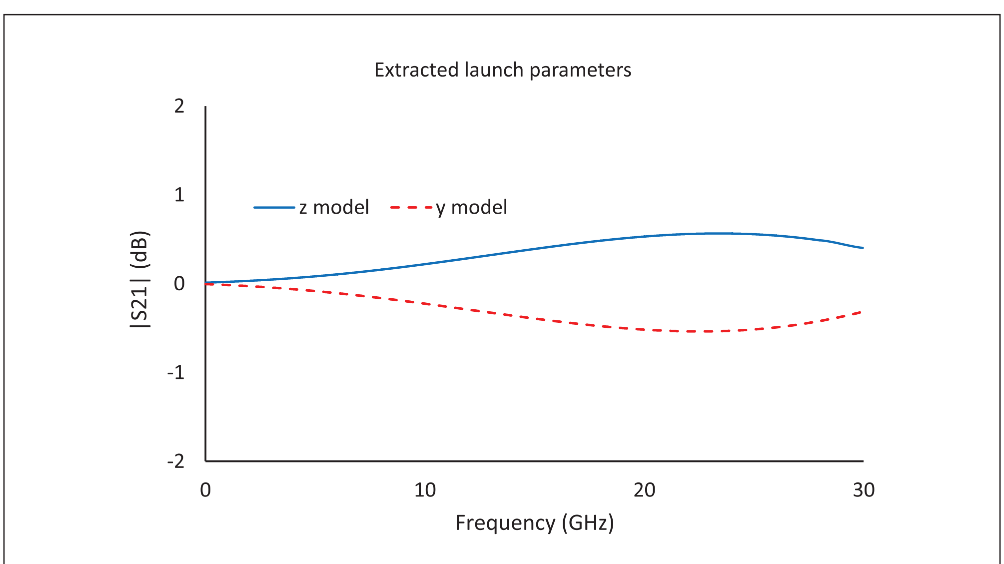

Figure 8. The extracted lumped element model behavior of the coaxial launch is plotted here for both cases (assuming it was a series Z model or a shunt Y model). Physically, the launch is better modeled as a shunt Y element (and largely capacitive).

If one were to just de-embed both launches, the net DUT return loss actually worsens as shown below. Since just those two lumped admittances do not characterize an electrically long fixture (with a big internal transition), this is perhaps not surprising.

Next, the via transition is analyzed with the peeling process. Again, it is not immediately known what nature this structure will have but, based on dimensions, one might suspect a chance at it being inductive (series-Z). Indeed from the data, it seems this is a more physical representation with some higher order behaviors starting to appear above ~25 GHz.

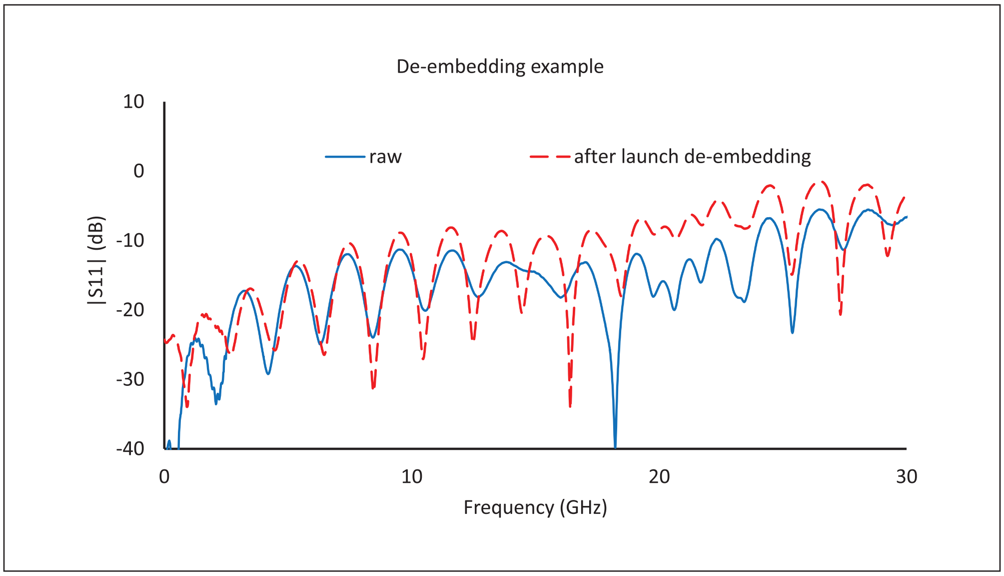

Figure 9. Just de-embedding the launches (ignoring transmission lines and the via) produced a worse result.

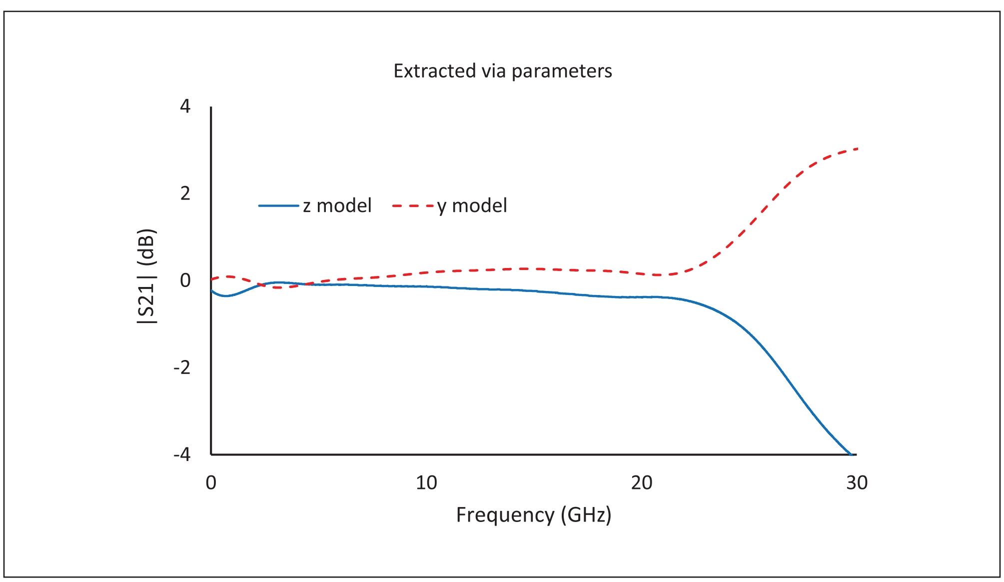

Figure 10. The extracted lumped element model behavior of the via is plotted here for both cases (assuming it was a series Z model or a shunt Y model). Physically, the via is better modeled as a series impedance (and largely inductive).

Combining the launch and via models with the transmission line segments of the fixture (just using the de-embedding engine's model based on physical length and known material properties), one does achieve a more believable de-embedded result:

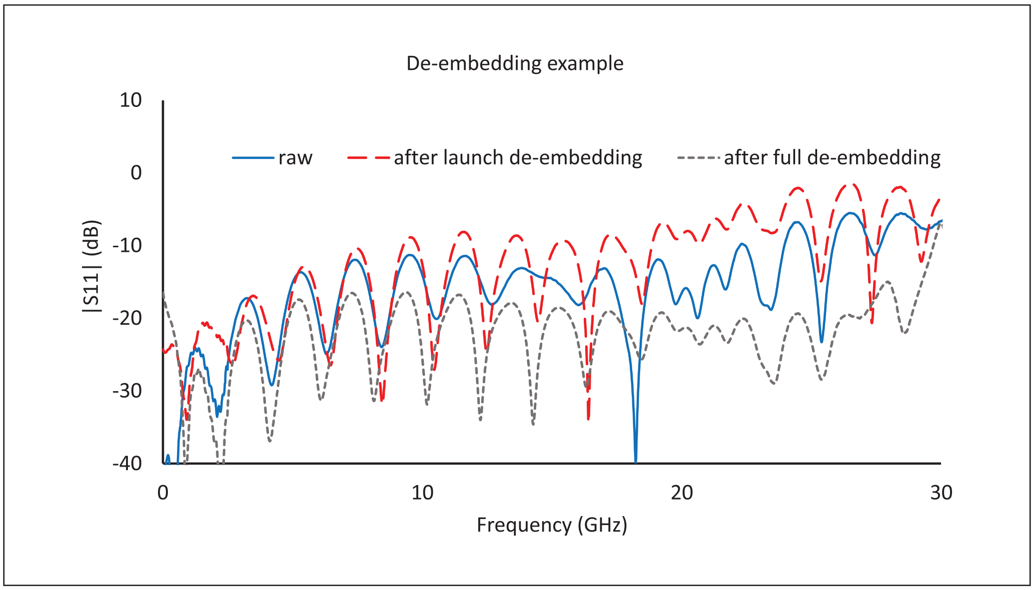

Figure 11. With the more complete description of the fixture now available, the de-embedding produced a more physical result.

It should be cautioned that this example worked out reasonably well because the losses and reflection levels of the fixture were not extremely high, the fixture was sufficiently long (about 500 ps long relative to a frequency range of about 30 GHz and a step size of 10 MHz), the DUT characteristics were completely incompatible with those of the fixture.

Summary

Sequential peeling is a model/measurement-based method at network extraction for de-embedding. It uses isolatable phase responses of defects to create a lumped-element description of a structure (shunt, series, or cross-bar) that can be physically meaningful and useful in sequential de-embedding. The method works best when the significant reflections are electrically small and isolated and the overall loss of the fixture is not too great but there are corrections available to help with the loss element.

References

[1] Se-Jung Moon; Xiaoning Ye; and Rex Smith, “Comparison of TRL calibration vs. 2x thru de-embedding methods,” 2015 IEEE Symposium on Electromagnetic Compatibility and Signal Integrity Proc., Jun. 2015, pp. 176 – 180.

[2] W.-C. Chang, G. J. Wunsch, and D. H. Schaubert, “Back-to-back measurement for characterization of phase-array antennas,“ IEEE Trans. Ant. Prop., vol. 48, pp. 1079-1085, July 2000.

[3] S. R. Pennock, C. M. D. Rycroft, P. R. Shepard, and T. Rozzi, “Transition characterization for de-embedding purposes,” Proc. European Micr. Conf., Oct. 1987, pp. 355-360.

[4] G. F. Engen, “An evaluation of the ‘back-to-back’ method of measuring adaptor efficiency,” IEEE Trans. Instrum. Meas., vol. 19, pp. 18-22, Feb. 1970.

[5] Jack Carrel, Heidi Barnes, Robert Sleigh, Hoss Hakimi, Mike Resso, “De-Mystifying the 28 Gb/s PCB Channel: Design to Measurement,” DesignCon 2014, Jan. 2014, pp. 1-27.

[6] J. Martens, “Simplified de-embedding techniques: some effects of match and geometry assumptions,” DesignCon 2015, Jan. 2015, pp. 1-18.

[7] D. DeGroot, K. Doshi, D. Dunham, and P. Pupalaikis, “De-embedding in High Speed Design,” 2012 DesignCon Proc., pp. 1-45, Jan. 2012.

[8] C.-J. Ong, A. Tripathi, D. Miller, and L. Tsang, “De-embedding a device-under-test (DUT) using thru’ measurements,” 2003 Electrical Performance In Electronic Packaging Conf. Proc., pp. 1-4, Oct. 2003.

[9] “VectorStar MS464XB: Calibration and Measurement Guide”, Anritsu publication 10410-00318H, Apr. 2017, Chps. 8, 10 and 22.

Anritsu envision : ensure

Specifications are subject to change without notice.

• United States
Anritsu Company
1155 East Collins Boulevard, Suite 100,
Richardson, TX, 75081 U.S.A.
Toll Free: 1-800-267-4878
Phone: +1-972-644-1777
Fax: +1-972-671-1877

• Canada
Anritsu Electronics Ltd.
700 Silver Seven Road, Suite 120,
Kanata, Ontario K2V 1C3, Canada
Phone: +1-613-591-2003
Fax: +1-613-591-1006

• Brazil
Anritsu Electrônica Ltda.
Praça Amadeu Amaral, 27 - 1 Andar
01327-010 - Bela Vista - Sao Paulo - SP - Brazil
Phone: +55-11-3283-2511
Fax: +55-11-3288-6940

• Mexico
Anritsu Company, S.A. de C.V.
Av. Ejército Nacional No. 579 Piso 9, Col. Granada
11520 México, D.F., México
Phone: +52-55-1101-2370
Fax: +52-55-5254-3147

• United Kingdom
Anritsu EMEA Ltd.
200 Capability Green, Luton, Bedfordshire LU1 3LU, U.K.
Phone: +44-1582-433280
Fax: +44-1582-731303

• France
Anritsu S.A.
12 avenue du Québec, Batiment Iris 1-Silic 612,
91140 Villebon-sur-Yvette, France
Phone: +33-1-60-92-15-50
Fax: +33-1-64-46-10-65

• Germany
Anritsu GmbH
Nemetschek Haus, Konrad-Zuse-Platz 1
81829 München, Germany
Phone: +49-89-442308-0
Fax: +49-89-442308-55

• Italy
Anritsu S.r.l.
Via Elio Vittorini 129, 00144 Roma Italy
Phone: +39-06-509-9711
Fax: +39-06-502-2425

• Sweden
Anritsu AB
Kistagången 20B, 164 40 KISTA, Sweden
Phone: +46-8-534-707-00
Fax: +46-8-534-707-30

• Finland
Anritsu AB
Teknobulevardi 3-5, FI-01530 VANTAA, Finland
Phone: +358-20-741-8100
Fax: +358-20-741-8111

• Denmark
Anritsu A/S
Kay Fiskers Plads 9, 2300 Copenhagen S, Denmark
Phone: +45-7211-2200
Fax: +45-7211-2210

• Russia
Anritsu EMEA Ltd.
Representation Office in Russia
Tverskaya str. 16/2, bld. 1, 7th floor.
Moscow, 125009, Russia
Phone: +7-495-363-1694
Fax: +7-495-935-8962

• Spain
Anritsu EMEA Ltd.
Representation Office in Spain
Edificio Cuzco IV, Po. de la Castellana, 141, Pta. 5
28046, Madrid, Spain
Phone: +34-915-726-761
Fax: +34-915-726-621

• United Arab Emirates
Anritsu EMEA Ltd.
Dubai Liaison Office
P O Box 500413 - Dubai Internet City
Al Thuraya Building, Tower 1, Suite 701, 7th floor
Dubai, United Arab Emirates
Phone: +971-4-3670352
Fax: +971-4-3688460

• India
Anritsu India Pvt Ltd.
2nd & 3rd Floor, #837/1, Binnamangla 1st Stage,
Indiranagar, 100ft Road, Bangalore - 560038, India
Phone: +91-80-4058-1300
Fax: +91-80-4058-1301

• Singapore
Anritsu Pte. Ltd.
11 Chang Charn Road, #04-01, Shriro House
Singapore 159640
Phone: +65-6282-2400
Fax: +65-6282-2533

• P. R. China (Shanghai)
Anritsu (China) Co., Ltd.
27th Floor, Tower A,
New Caohejing International Business Center
No. 391 Gui Ping Road Shanghai, Xu Hui Di District,
Shanghai 200233, P.R. China
Phone: +86-21-6237-0898
Fax: +86-21-6237-0899

• P. R. China (Hong Kong)
Anritsu Company Ltd.
Unit 1006-7, 10/F., Greenfield Tower, Concordia Plaza,
No. 1 Science Museum Road, Tsim Sha Tsui East,
Kowloon, Hong Kong, P. R. China
Phone: +852-2301-4980
Fax: +852-2301-3545

• Japan
Anritsu Corporation
8-5, Tamura-cho, Atsugi-shi,
Kanagawa, 243-0016 Japan
Phone: +81-46-296-6509
Fax: +81-46-225-8359

• Korea
Anritsu Corporation, Ltd.
5FL, 235 Pangyoyeok-ro, Bundang-gu, Seongnam-si,
Gyeonggi-do, 13494 Korea
Phone: +82-31-696-7750
Fax: +82-31-696-7751

• Australia
Anritsu Pty Ltd.
Unit 20, 21-35 Ricketts Road,
Mount Waverley, Victoria 3149, Australia
Phone: +61-3-9558-8177
Fax: +61-3-9558-8255

• Taiwan
Anritsu Company Inc.
7F, No. 316, Sec. 1, Neihu Rd., Taipei 114, Taiwan
Phone: +886-2-8751-1816
Fax: +886-2-8751-1817

CE nqa ISO 9001 Registered

11410-01036, Rev. A Printed in United States 2017-05